SIMULATIONS OF BEAM STRIKES ON ADVANCED PHOTON SOURCE UPGRADE COLLIMATORS USING FLASH, MARS, AND ELEGANT*

J. Dooling†, M. Borland, A. Grannan, C. Graziani, R. Lindberg, G. Navrotski
Argonne National Laboratory, Lemont, IL, USA
D. Lee, Y. Lee
University of California, Santa Cruz, CA, USA
N. Cook
RadiaSoft LLC, Boulder, CO, USA

Abstract

Modeling of high-energy-density electron beams on collimators proposed for the Advanced Photon Source Upgrade (APS-U) storage ring (SR) is carried out with codes FLASH, MARS, and elegant. Simulations are compared with experimental data from two separate beam dump studies conducted in the present APS SR. Whole beam dumps of the 6-GeV, 200-mA (736-nC), ultra-low emittance beam will deposit acute doses of 30 MGy within 10-20 microseconds, leading to hydrodynamic behavior in the collimator material. Goals for coupling the codes include accurate modeling of hydrodynamic behavior, methods to mitigate damage, and understanding the effects of the resulting shower downstream of the collimator. Experiments, though valuable, are difficult and expensive to conduct. The coupled codes will provide a method to model differing geometries, materials, and loss scenarios. Efforts thus far have been directed toward using FLASH to reproduce observed damage seen in aluminum test pieces subjected to varying beam strike intensities. Stabilizing the Eulerian mesh against large energy density gradients as well as establishing release criteria from solid to fluid forms are discussed.

INTRODUCTION

Simulations with the particle-matter interaction program MARS [1], using loss distributions obtained with the electron-beam-dynamics code elegant [2,3], indicated that unplanned beam aborts could lead to damage of collimators proposed for the Advanced Photon Source Upgrade (APS-U) storage ring (SR) [4]. The low-emittance beam leads to high-energy-density (HED) conditions in the struck material. Electron flux and dose distributions for a 15.3-nC, 6-GeV bunch striking an idealized collimator at the inboard apex are plotted in Fig. 1. The apex is the point of the collimator closest to the beam centerline; in the present model, the inboard apex is located at $x = -0.42$ cm. The collimators are modeled with a horizontal radius of 0.865 m.

Using a configuration designed to emulate APS-U conditions [5], experiments were conducted to test this result by dumping up to 200 mA on aluminum collimator test pieces. A diagnostic camera recording visible radiation from the
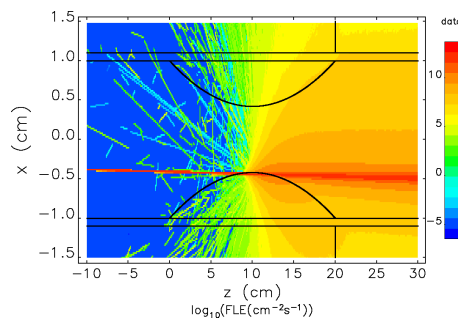
(a) Electron-positron flux.
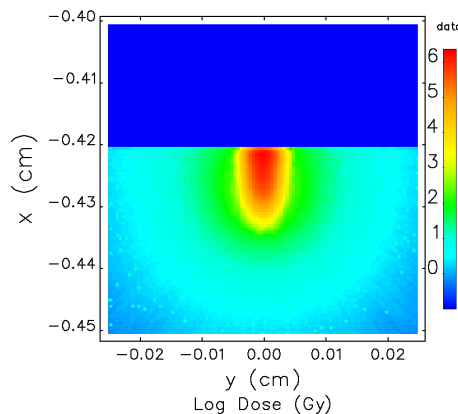
(b) Dose at the collimator apex.

Figure 1: (a) Electron-positron flux and (b) transverse dose map for a single 15.3-nC, 6-GeV bunch striking the collimator apex. The bunch is one in a 48-bunch pattern comprising a storage-ring current of 200 mA.

collimator showed bright emission during beam strikes; this data has been previously presented [6,7]. Figure 2 shows a post-experiment photograph of one of the two collimator test pieces, confirming damage to the test piece beginning at 32 mA. The data in Fig. 3 is part of the set used to benchmark the hydrodynamic simulations discussed below.

Coupling of hydrodynamic and particle-matter codes have been carried out by a number of researchers [9–12]; these have all been simulations of proton beams striking 2-D cylindrical targets. Hydrodynamics was modeled using commercially available Lagrangian solvers in all but the first case. In the present effort, the Eulerian hydrodynamics code, FLASH is employed [13,14]. FLASH is a radiation MHD

MC2: Photon Sources and Electron Accelerators
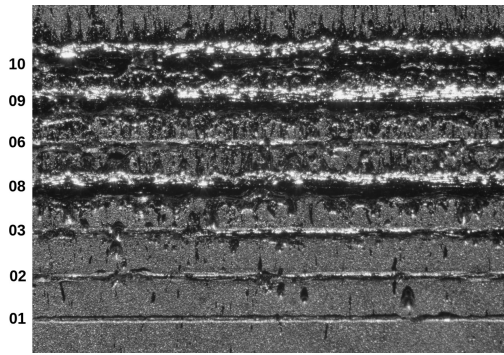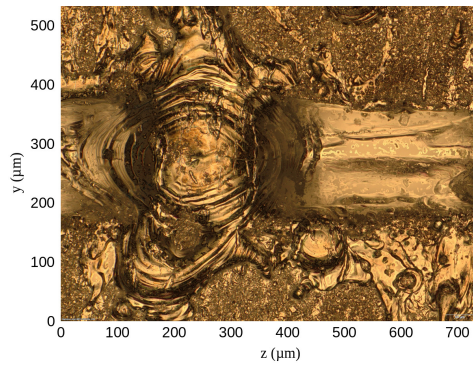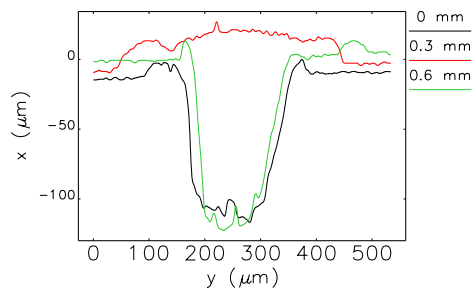
A04 Circular Accelerators

Figure 2: Post-irradiation image of one of two aluminum collimator test pieces. Numbers listed to the left of the photograph are sequence numbers and represent beam dump currents as follows: 01: 34.6, 02: 69.4, 03: 99.1, 06: 100.0, 08: 202.0, 09: 201.2, and 10: 202.1 mA. The vertical separation between adjacent strike tracks is 0.4 mm [8].

(a) Microscopy.

(b) Height profiles.

Figure 3: (a) Microscopy of strike 8 shown in Fig. 2 in a 0.7-mm length near the collimator apex [8]. (b) height profiles in the y-direction across the strike zone at z = 0, 0.3 and 0.6 mm. The hill feature between z = 0.1 mm and 0.3 mm across the strike trench is of note [8].

Eulerian hydrodynamics solver using adaptive mesh refinement (AMR).

HYDRODYNAMIC SIMULATIONS

Physical Considerations

The FLASH code is designed to treat all material in the domain as a fluid; there are no default characterizations for a metal, plastic, or crystalline structure. Thermal stress, deformation, and plastic flow are unaccounted for by FLASH's core hydrodynamics and MHD solvers [15, 16] used in this study. As a result, we must carefully choose conditions under which the metallic target behaves like a fluid, and introduce constraints on density flows when these conditions are not satisfied.

Release Conditions

Our solution is to apply a special condition to the metal, simulated using the so-called "BDRY_VAR" variable in FLASH, which treats the aluminum target as non-stationary solid material cells. This approach prevents the solid aluminum target from the standard hydrodynamical fluid flow updates (i.e., advection) while retaining all relevant thermal transport conditions. For the specific conditions, electron temperatures and internal energies may still be incremented through the application of an effective dose map, and subsequent heat exchange between electrons and ions, as well as thermal diffusion outward from the location of deposition, will occur. In this way, we can dynamically capture the localized heating and cooling of the metal region while retaining its density at low temperatures.

The challenge to this approach is in determining a transition point, beyond which the material will move like a fluid. We have chosen to use the local electron temperature to set such a "release" condition, using the melting point and heat of vaporization for Aluminum to identify potential candidates for this temperature condition. For the range of densities and initial conditions on temperature and pressure, we have considered release conditions ranging from the vaporization temperature of Al, T_{vap} (2743 K) through $8T_{vap}$, representing an eight-fold dynamic range.

Hydrodynamics Advection Solver

Two common options for improving stability include (1) reducing the time step to better resolve large fluxes, and (2) reducing the interpolation order in the hydro solver, to reduce gradients in the fluid flow. Both approaches are closely related to increasing numerical dissipation. In our simulations, both approaches have effect on fidelity but they come at a price. The first approach increases computational costs and the latter approach reduces local fidelity by dropping the solution accuracy. In order to balance the deleterious effects of each approach, we have implemented a hybrid scheme, wherein the solver interpolation order and time step are reduced during the deposition, before returning to their original state. This approach has produced more consistent performance.

MC2: Photon Sources and Electron Accelerators

A04 Circular Accelerators

Boundary Conditions

A final concern addressed during the work thus far is the choice of boundary conditions in the simulation domain. Boundary conditions are important for preserving self-consistency in regions of significant fluid outflow or temperature gradients. While the relative importance of the boundary can be reduced by increasing domain size, this comes at the cost of increased computational expense. This increased expense is compounded for 3D simulations.

Our studies demonstrate that the most important boundary for our simulations is the right-side boundary (opposite the metal surface), through which most of the fluid and energy leaves the domain. While the choice of hydro boundaries is straightforward (we apply an "outflow" condition to permit material to leave the domain with no impact on the remaining fluid), the choice of boundaries for the diffusion solver is less obvious. A Dirichlet boundary enforces a flux magnitude condition, which is suitable if the temperature equilibrates rapidly along the boundary region, whereas a Neumann condition enforces a a constant flux-gradient and is thus more appropriate if the boundary region is expected to remove heat at a consistent rate.

Results

A 2-D FLASH simulation output of a 200-mA, 6-GeV beam striking at the collimator apex is presented in Fig. 4. The fill pattern is 972 bunches of equal charge. With the SR harmonic number of 1296, this means 3 of every 4 rf buckets are filled with charge. The 2-D image is oriented such that the aluminum collimator is on the left and vacuum of the beam chamber is on the right. The simulation shows the condition at the end of the 3-turn strike period where 1 turn in the APS SR is 3.68 μs. *x*- and *y*-density profiles in the strike zone along the paths shown in Fig. 4 are plotted in Fig. 5.

Of interest is the collimator material released into the vacuum chamber during the beam strike. This fluid material will interact with the electron beam yet to strike the collimator. An example of this behavior is given in Fig. 6.
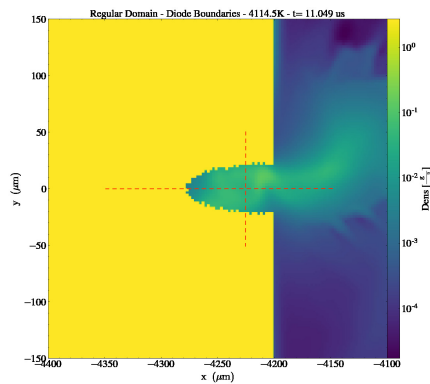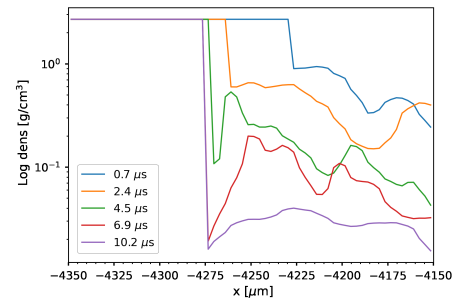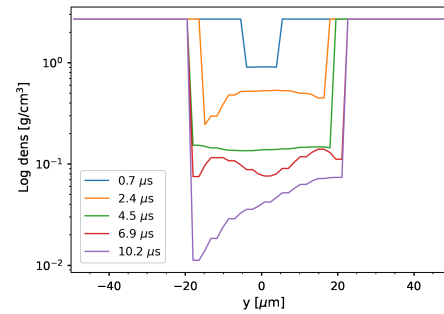

Figure 4: 2-D FLASH simulation of collimator density after a 972-bunch, 6-GeV, 200-mA beam strike.

(a) *x* profiles.

(b) *y* profiles.

Figure 5: Al density profiles from FLASH at given times in (a) x and (b) y for the 200-mA beam result along the dotted lines shown in Fig. 4.
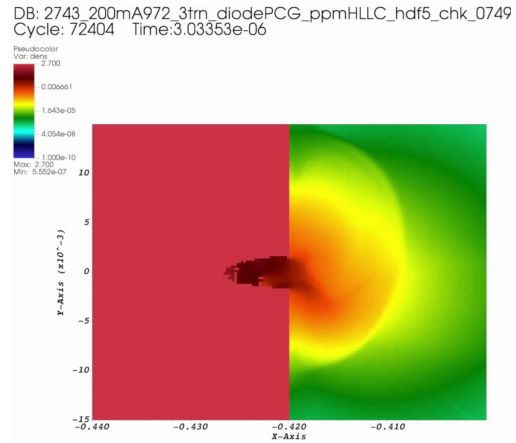

Figure 6: 2-D FLASH simulation showing collimator fluid density after release flowing into the vacuum chamber. The time of the density map is 3.1 μs or just under 1 turn in a loss event covering 3 turns.

SUMMARY

We have begun the process of modeling the effects of HED electron beams striking collimators during whole beam dumps. We have made progress defining the release condition that matches experimental observations; presently the release condition temperature that best matches the data is in the range of $1.0 - 1.5 T_{vap}$. The next steps in this work are to provide modified density maps for MARS and verify 3-D simulations.

MC2: Photon Sources and Electron Accelerators

A04 Circular Accelerators

REFERENCES

[1] N. V. Mokhov and S. I. Striganov, "MARS15 Overview", in *AIP Conference Proceedings*, Batavia, Illinois, USA, Sep. 2007, pp. 50–60. `doi:10.1063/1.2720456`

[2] M. Borland, "elegant: A Flexible SDDS-Compliant Code for Accelerator Simulation", ANL, Lemont, Illinois, USA, Rep. LS-287, Sep. 2000.

[3] Y. Wang and M. Borland, "Pelegant: A Parallel Accelerator Simulation Code for Electron Generation and Tracking", in *AIP Conference Proceedings*, Lake Geneva, Wisconsin, USA, Jul. 2006, p. 241.

[4] M. Borland *et al.*, "The Upgrade of the Advanced Photon Source", in *Proc. 9th Int. Particle Accelerator Conf. (IPAC'18)*, Vancouver, Canada, Apr.-May 2018, pp. 2872–2877. `doi:10.18429/JACoW-IPAC2018-THXGBD1`

[5] M. Borland, J. C. Dooling, R. R. Lindberg, V. Sajaev, and Y. P. Sun, "Simulation of Beam Aborts for the Advanced Photon Source to Probe Material-Damage Limits for Future Storage Rings", in *Proc. North American Particle Accelerator Conf. (NAPAC'19)*, Lansing, MI, USA, Sep. 2019, paper MOPLM07, pp. 106–109. `doi:10.18429/JACoW-NAPAC2019-MOPLM07`

[6] J. C. Dooling *et al.*, "Diagnostics for Collimator Irradiation Studies in the Advanced Photon Source Storage Ring", in *Proc. 9th Int. Beam Instrumentation Conf. (IBIC'20)*, Santos, Brazil, Sep. 2020, pp. 26–33. `doi:10.18429/JACoW-IBIC2020-TUAO02`

[7] J. C. Dooling *et al.*, "Studies of Beam Dumps in Candidate Horizontal Collimator Materials for the Advanced Photon Source Upgrade Storage Ring", in *Proc. North American Particle Accelerator Conf. (NAPAC'19)*, Lansing, MI, USA, Sep. 2019, paper MOPLM14, pp. 128–131.

[8] J. Dooling *et al.*, "Collimator Irradiation Studies in the Advanced Photon Source at Energy Densities Expected in Next-Generation Storage Ring Light Sources", submitted for publication.

[9] D. C. Wilson, R. P. Godwin, J. C. Goldstein, N. V. Mokhov, and C. A. Wingate, "Hydrodynamic Calculations of 20-TeV Beam Interactions with the SSC Beam Dump", in *Proc. 15th Particle Accelerator Conf. (PAC'93)*, Washington D.C., USA, Mar. 1993, pp. 3090–3093. `http://accelconf.web.cern.ch/p93/PDF/PAC1993_3090.PDF`

[10] N. A. Tahir, F. Burkart, R. Schmidt, A. Shutov, and A. R. Piriz, "Review of hydrodynamic tunneling issue in high power particle accelerators", *Nuclear Inst. and Methods in Physics Research B*, vol. 427, pp. 70–86, 2018. `doi:10.1016/j.nimb.2018.04.009`

[11] M. Scapin, L. Peroni, V. Boccone, and F. Cerutti, "Effects of high-energy intense multi-bunches proton beam on materials", *Computers and Structures*, vol. 141, pp. 74–83, 2014. `doi:10.1016/j.compstruc.2014.05.008`

[12] Y. Nie *et al.*, "Simulation of hydrodynamic tunneling induced by high-energy proton beam in copper by coupling computer codes", *Phys. Rev. Accel. Beams*, vol. 22, p. 014501, 2019. `doi:10.1103/PhysRevAccelBeams.22.014501`

[13] B. Fryxell *et al.*, "FLASH: An Adaptive Mesh Hydrodynamics Code for Modeling Astrophysical Thermonuclear Flashes", *Astrophysical Journal Supp. Series*, vol. 131, pp. 273–334, Nov. 2000. `doi:10.1086/317361`

[14] P. Tzeferacos *et al.*, "Laboratory evidence of dynamo amplification of magnetic fields in a turbulent plasma", *Nat. Comm.*, vol. 9, p. 591, Feb. 2018. `doi:10.1038/s41467-018-02953-2`

[15] D. Lee and A. E. Deane, "An unsplit staggered mesh scheme for multidimensional magnetohydrodynamics", *Journal of Computational Physics*, vol. 228, pp. 952–975, 2009. `doi:10.1016/j.jcp.2008.08.026`

[16] D. Lee, "A solution accurate, efficient and stable unsplit staggered mesh scheme for three dimensional magnetohydrodynamics", *Journal of Computational Physics*, vol. 243, pp. 269–292, 2013. `doi:10.1016/j.jcp.2013.02.049`